

Revised Estimates of Ocean Surface Drag in Strong Winds

M. Curcic¹ and B. K. Haus¹

¹Rosenstiel School of Marine and Atmospheric Science, University of Miami, 4600 Rickenbacker Causeway, Miami, FL 33149.

Key Points:

- New laboratory experiments confirm presence of air-sea drag saturation in strong winds
- Previous laboratory drag data found to be underestimated due to an error in scaling to 10-m height
- Corrected data show air-sea drag saturation at 34% higher magnitude and 12% lower wind speed

arXiv:2002.10590v1 [physics.ao-ph] 24 Feb 2020

Corresponding author: Milan Curcic, mcurcic@miami.edu

Abstract

Air-sea drag governs the momentum transfer between the atmosphere and the ocean, and remains largely unknown in hurricane-force winds. We revisit the momentum budget and eddy-covariance methods to estimate the surface drag coefficient in the laboratory. Our drag estimates agree with field measurements in low-to-moderate wind speeds, and previous laboratory measurements in hurricane-force winds. The drag coefficient saturates at 2.6×10^{-3} and $U_{10} \approx 25 \text{ m s}^{-1}$, in agreement with previous laboratory results. During the analysis of the data, we discovered an error in the scaling to 10-m winds in the original source code used by Donelan et al. (2004). We present the corrected data and describe the correction procedure. Although the correction to the data does not change the key finding that the drag saturates in strong winds, the magnitude and the wind speed threshold of drag saturation are significantly changed. We recommend that the correction be applied to any surface flux parameterization schemes in weather and ocean prediction models that relied on the original laboratory data.

Plain Language Summary

We measure the rate of air-sea momentum transfer (surface drag) in strong winds in a 15-m long wind-wave tank. In support of previous work, we find further evidence that the drag saturates (levels off) in hurricane-force winds, based on three different measurement methods. The level of drag saturation, however, is higher than previously thought. The leading study that discovered the drag saturation in high winds had an error in the source code used for the analysis of the data. This error resulted in an overestimate of 10-m wind speed, and an underestimate of the drag coefficient. This finding is important because previous laboratory data that underestimate the drag were used to implement surface flux parameterization in the most widely used research and operational weather prediction model for tropical cyclone applications.

1 Introduction

Air-sea drag determines the rate of vertical exchange of horizontal momentum between the atmosphere and the ocean (Phillips, 1966; Large & Pond, 1981; Edson et al., 2013). This exchange is mediated largely by ocean surface waves (Donelan et al., 1993, 1997), and in the most extreme weather conditions by bubbles, spray, and spume (Andreas, 1992; Holthuijsen et al., 2012). Correct formulation of the air-sea momentum flux as a surface boundary condition is critical for numerical weather (Powers et al., 2017; Skamarock et al., 2012, 2018) and ocean prediction models (Shchepetkin & McWilliams, 2005; Chassignet et al., 2007). This is especially true for the prediction of extreme weather events such as hurricanes and winter storms (Chen & Curcic, 2016) where strong winds, high waves, and surge compound to devastating effects on coastal communities.

Air-sea drag is challenging to measure in hurricanes because of their transient and destructive nature. To date, in situ measurements remain sparse and limited to tropical storm-force winds ($U_{10} < 27 \text{ m s}^{-1}$, Potter et al. (2015)). Other estimates of drag in the field are limited to indirect measurement techniques, including the profile method using GPS dropsondes (Powell et al., 2003; Holthuijsen et al., 2012), angular momentum budget (Bell et al., 2012), and upper-ocean momentum budget (Jarosz et al., 2007; Sanford et al., 2011; Hsu et al., 2019). These estimates come with significant variability, possibly due to limited sample sizes, indirect measurement methods, and drag dependence on wave-state. Alternatively, drag can be measured in high winds in a controlled laboratory environment (Donelan et al., 2004; Takagaki et al., 2012, 2016; Donelan, 2018). Current consensus from laboratory and field data is that the

drag coefficient likely saturates in hurricane-force winds, and perhaps even decreases in more extreme conditions (Holthuijsen et al., 2012; Soloviev et al., 2014; Donelan, 2018).

The main limitation of all laboratory drag estimates in high winds is extremely short fetch, which caps the level of wave development that can be achieved in wind-wave tanks. Thus, these conditions are not equivalent to those in the field: In the laboratory, hurricane-strength winds are forced over calm water, and measurements are taken at fetch typically less than 10 m (Donelan et al., 2004; Takagaki et al., 2012); in contrast, hurricane winds in the field are coupled with complex and mature wave spectra that develop over fetches of order 100 km (Wright et al., 2001; Chen & Curcic, 2016; Curcic et al., 2016; Collins et al., 2018). Despite these limitations, the data collected by Donelan et al. (2004) were implemented as surface flux parameterization in the Weather Research and Forecasting (WRF, Powers et al. (2017)) model, and recommended for tropical cyclone applications by Davis, Wang, et al. (2008). Specific values of drag measured in the laboratory have thus had direct impact on weather and ocean prediction in both research and operational settings.

In this study, we re-evaluate the drag coefficient in high winds over initially calm water similarly to Donelan et al. (2004) and Takagaki et al. (2012). We estimate the drag using the eddy-covariance flux method (Tennekes et al., 1972; Edson et al., 1998) and the momentum budget method (Donelan et al., 2004) in 10-m wind speeds up to 50 m s^{-1} , in fresh and seawater. Our main objective is to validate the momentum budget method and reproduce the drag saturation results by Donelan et al. (2004) in the same wind-wave tank as the original study. We repeat the experiment with more and newer instruments, in both fresh and seawater, and calculate the error estimates for both eddy-covariance and momentum budgeted methods. During our data analysis, we identified a programming error in the original source code by Donelan et al. (2004), which was used to scale the in situ wind speed to a reference height of 10 m. The error caused an overestimate of 10-m wind speed and an underestimate of the drag coefficient. We include the corrected drag coefficient values alongside our new results. This study addresses the need to identify and better understand the limitations of drag measurements in wind-wave flumes, and help interpret how the laboratory results can be applied to air-sea processes in the field and numerical models.

2 The Momentum Budget in the Laboratory

We conducted the experiments in the Air-Sea Interaction Salt-Water Tank (ASIST) at the University of Miami. This tank has been successfully used to measure air-sea fluxes (Donelan et al., 2004; Donelan, 2018; Jeong et al., 2012), wave modulation (Donelan et al., 2010; Laxague et al., 2017), and sea-spray generation (Ortiz-Suslow et al., 2016), among others. The tank is 15-m long with a $1 \times 1 \text{ m}$ cross-section. The final 5 m of the tank feature a sloping porous beach designed to dissipate waves while minimizing shoaling and reflection. The laboratory set-up and the position of instruments are illustrated in Fig. 1.

We follow the momentum budget approach by Donelan et al. (2004) to estimate drag in high winds. These conditions are prohibitive to the eddy-covariance method due to copious spray that corrupts the measurement. The momentum budget method in the tank is based on the steady-state momentum balance between surface stress τ , mean slope of the water surface $\frac{\partial \eta}{\partial x}$, radiation stress gradient $\frac{\partial S_{xx}}{\partial x}$, air pressure gradient $\frac{\partial p_a}{\partial x}$, and the bottom stress τ_b :

$$\tau = \rho_w g h \frac{\partial \eta}{\partial x} + \frac{\partial S_{xx}}{\partial x} + h \frac{\partial p_a}{\partial x} + \tau_b \quad (1)$$

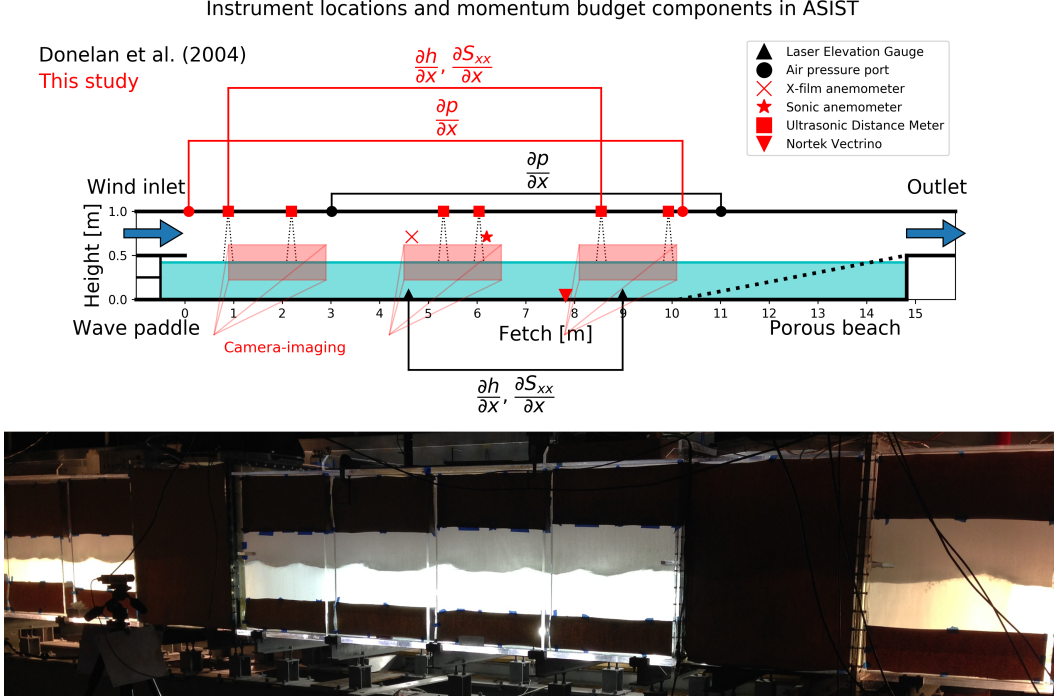


Figure 1. (Top) Laboratory set up and locations of instruments in the tank from Donelan et al. (2004) (black) and this study (red). Connecting lines indicate the instrument positions used to compute pressure, elevation, and radiation stress gradients. (Bottom) Photograph of the ASIST wave tank during the experiment.

where ρ_w and h are water density and mean water height, respectively, g is gravitational acceleration, η is the water elevation relative to the resting water height. Specific locations in the tank over which the gradients are calculated for both this and the reference study (Donelan et al., 2004) are shown in Fig. 1. Sampling the whole length of the tank is important because $\partial p/\partial x$ and $\partial \eta/\partial x$ may vary in the along-tank direction. Thus, if we measure water elevation and air pressure in multiple locations in the tank, and have an estimate of the bottom stress, then we can calculate the surface stress using Eq. 1. Drag coefficient at the reference height of 10 m is then $\tau/(\rho_a U_{10}^2)$, where ρ_a is air density and U_{10} is wind speed at 10 m.

We measure the eddy-covariance momentum flux using a TSI hot-film anemometer at 4.7 m fetch, and a Campbell Scientific IRGASON sonic anemometer at 6.1 m fetch. We calibrated the hot-film anemometer using a pitot tube mounted at the same fetch and height, which measured the horizontal component of the wind. The air pressure gradient was measured via two small holes in the ceiling at 0.1 m and 10.2 m fetch. The mean water elevation was measured using Senix ultrasonic distance-meters mounted at the ceiling and looking down at the water surface. The mean surface slope and radiation stress gradient were calculated by taking the difference between the data at 8.6 m and 0.9 m fetch. This yields a control section of 7.7 m, in contrast to 4.4 m in the momentum budget set-up by Donelan et al. (2004). In addition, we use high-speed cameras to film the water interface at three 2 m-long sections of the tank (0.9-2.9, 4.5-6.5, and 8.1-10.1 m fetch) (Fig. 1, bottom). We followed the image processing method by Laxague et al. (2017) to extract the wave frequency spectra and significant wave height as function of fetch. Finally, we mounted a Nortek Vectrino at 7.8 m fetch to measure 3-dimensional water velocity in the lower 4 cm profile, which provided an

estimate of the bottom stress τ_b . All measurements are averaged over 6-minute runs, following Donelan et al. (2004). We propagate the instrument errors in our analysis to calculate the final error bars for the drag coefficient.

We collected all data in 13 different wind conditions, from calm to approximately 25 m s^{-1} (centerline, $z = 0.29 \text{ m}$) in equal 6-minute increments, in fresh and seawater. The resting water depth was 0.42 m in all experiments. This laboratory set-up enables: (a) direct comparison with previous laboratory measurements (Donelan et al., 2004; Takagaki et al., 2012) and observing the drag saturation; and (b) testing the momentum budget, eddy-covariance, and side-camera imaging techniques for application in larger wind-wave flumes.

3 Drag Coefficient in High winds

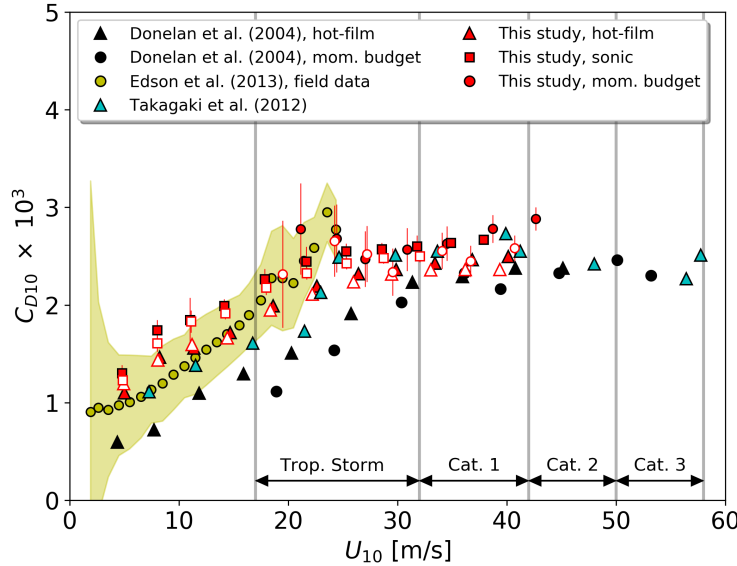


Figure 2. Drag coefficient scaled to 10-m height from eddy covariance and momentum budget from Donelan et al. (2004) and this study, laboratory data from Takagaki et al. (2012), and field measurements from Edson et al. (2013). Error bars from our study denote instrument error and/or method uncertainty. Field data are binned averages \pm one standard deviation, and denote uncertainty from instrument errors and natural variability. Data from Donelan et al. (2004) are shown in black. Solid and open markers from this study are from freshwater and seawater experiments, respectively. Vertical lines separate different Saffir-Simpson tropical cyclone intensity categories.

We first evaluate the drag coefficient as function of wind speed, based on measurements from the new experiments in the ASIST laboratory (Fig. 2). We compute the drag coefficient from three sources: Hot-film and sonic anemometers using the eddy-covariance method, and the momentum budget method. To evaluate the robustness between separate experiments, we include both the data from freshwater (solid markers) and seawater (open markers). Unlike previous laboratory data, we calculate the error bars associated with instrument accuracy and uncertainty of the momentum

budget method. For reference, we compare our results with the data from the field (Edson et al., 2013) and laboratory (Donelan et al., 2004; Takagaki et al., 2012).

There are three key takeaways from Fig. 2. First, our new data confirm the presence of drag saturation in high winds. The drag coefficient increases with wind speed up to $U_{10} \approx 25 \text{ m s}^{-1}$, at a level of $C_D \approx 2.5 \times 10^{-3}$, in agreement with the laboratory data by Takagaki et al. (2012). Stress measured by the sonic anemometer (fetch of 6.1 m) is consistent with that measured by Takagaki et al. (2012) (fetch of 6 m), and both are slightly higher relative to the stress measured with the hot-film anemometer (fetch of 4.7 m). The drag values are expected to be sensitive to fetch because the roughness elements are short wind-waves that grow downwind. Main hypotheses that attempt to explain drag saturation include separation of air-flow (sheltering) in the lee of steep wave crests (Donelan et al., 2004) and limited wave spectrum development due to wave breaking (Takagaki et al., 2012, 2016).

Second, drag coefficients from three different sources in new experiments are clustered together without notable outliers. The new data also fall largely within the window of natural variability of the field measurements in winds up to 25 m s^{-1} . In high winds, the drag coefficient is saturated between 2.3×10^{-3} and 2.9×10^{-3} , with an average value of 2.49×10^{-3} . The drag saturation signal is also consistent between fresh and seawater experiments. While the high-wind drag coefficient is slightly lower in seawater (2.41×10^{-3}) than in fresh water (2.58×10^{-3}), we do not explore these effects further in this paper. These results give us confidence in our instrumentation and the momentum budget method for evaluating drag, and suggest that the drag saturation signal is robust. The momentum budget errors decrease with wind speed because $\partial\eta/\partial x$ (along-tank slope) becomes significantly larger than the measurement error of η .

Finally, while we reproduce the drag saturation found by Donelan et al. (2004), their drag estimates are consistently lower than the new laboratory data, as well as field data (Edson et al., 2013) in low-to-moderate winds. In addition, their wind speed scaled to 10-m height extends considerably further (highest value of 54 m s^{-1}) relative to this study (highest value of 42 m s^{-1}). We did not initially expect this discrepancy considering that both this study and Donelan et al. (2004) used the same wind-wave tank, resting water depth, and wind forcing. The following section describes the source of the discrepancy and the proposed correction.

4 Correction to Drag and Wind Data by Donelan et al. (2004)

During the momentum budget analysis of the new laboratory data, we discovered a critical flaw in the original source code used to calculate drag coefficient values shown in Figure 2 of Donelan et al. (2004). The correction is straightforward and can be applied using existing data from the original experiment. We show the original and corrected drag coefficients by Donelan et al. (2004) in Fig. 3. Again, we show the field data by Edson et al. (2013) for reference. The correction brings the original drag coefficient saturation values from 2.24×10^{-3} to 3.01×10^{-3} , an increase of 34%. The saturation now occurs at lower wind speed, $U_{10} \approx 29 \text{ m s}^{-1}$ instead of $U_{10} \approx 33 \text{ m s}^{-1}$, a 12% decrease, which is consistent with both this study and Takagaki et al. (2012). Corrected drag coefficients are more consistent with the field data in the $15 - 23 \text{ m s}^{-1}$ range, as well as the new laboratory data from this study (Fig. 2). The WRF drag parameterization for the tropical flux configuration (Davis, Wang, et al., 2008), clearly modeled after the original laboratory data, inherited the underestimate of the drag saturation magnitude, and overestimate of the wind speed threshold at which the saturation occurs.

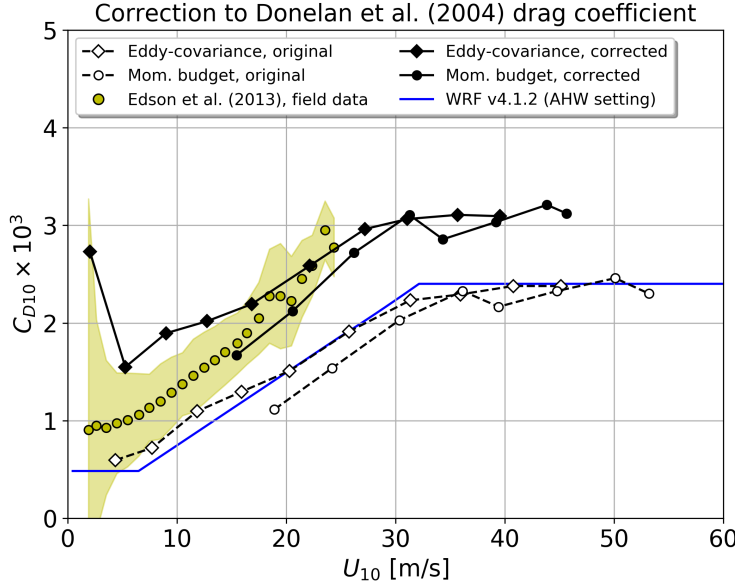


Figure 3. Original (black, dashed) and corrected (black, solid) drag coefficient data by Donelan et al. (2004). Field data (mean \pm one standard deviation) from Edson et al. (2013) are shown in yellow. Surface drag parameterization in WRF (Advanced Hurricane WRF setting) is shown in blue.

Where does the error in the drag coefficient by Donelan et al. (2004) come from? Wind and stress in the laboratory are measured at the height of the instrument, in this case 0.3 m. For convenience of comparison with prior work, field measurements, as well as for application to models, in situ wind and drag coefficient are commonly scaled to some reference height, typically 10 m above sea level for meteorological and oceanographic applications. Assuming neutral stability, the relationship is:

$$U_{10} = U_z + \frac{u_*}{\kappa} \log\left(\frac{10}{z}\right) \quad (2)$$

where U_z is the measured wind speed, u_* is the friction velocity, κ is the Von Kármán constant (0.4), and z is the height of the measurement (0.3 m). The drag coefficient scaled to 10-m height is then $(u_*/U_{10})^2$.

The values used for U_z in the original source code come from a different set of measurements (wind and stress profiles) and do not correspond to the runs during which the eddy-covariance and momentum budget data were collected. Fig. 4 shows that the wind speed extrapolated from profile measurements is considerably higher than the in situ $U_{0.3}$, measured by the pitot anemometer during the eddy-covariance and momentum budget runs. We also show the in situ-measured wind speed at 0.29 m height ($U_{0.29}$) from our study for comparison. $U_{0.29}$ from this study is marginally smaller than the pitot-measured $U_{0.3}$ from Donelan et al. (2004), primarily because the ASIST tank in 2003 was configured to recirculate the air, allowing for slightly higher wind speeds, and secondarily due to a small difference in measurement height. The stress measurements are thus unaffected by the error. The only aspects of the original study that are affected by the error are the values of wind and drag coefficient scaled to 10-m height. To correct the U_{10} and C_D estimates from eddy-covariance and momentum budget approaches by Donelan et al. (2004), compute the friction

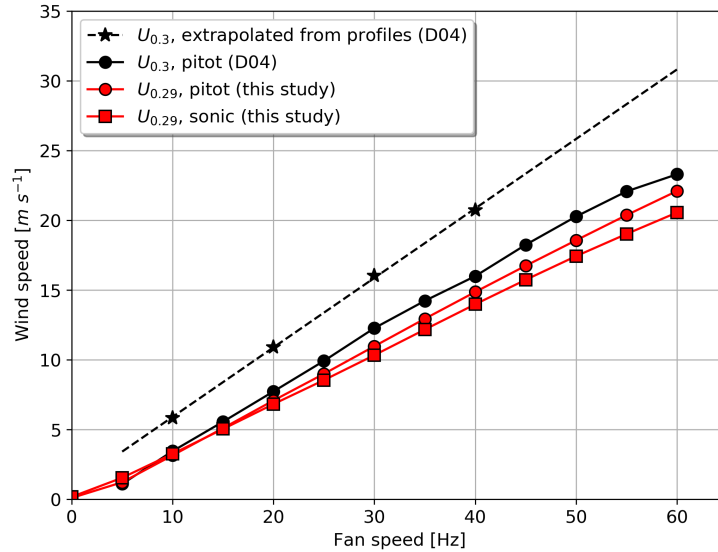


Figure 4. Extrapolated values (black stars) and in situ measurements (black circles) of $U_{0.3}$ from Donelan et al. (2004), and measured $U_{0.29}$ by pitot (red circles) and sonic (red squares) anemometers during this study, as function of tank fan speed.

velocity $u_* = \sqrt{C_D}U_{10}$, and compute the new values of U_{10} and C_D following Eq. (2), using in situ measured wind speed as U_z instead of that extrapolated from profile measurements. This correction results in a decrease in U_{10} and an increase in C_D , as shown in Fig. 4.

The error and the corresponding correction for the first time explain both the anomalously low values of C_D relative to the field data, and the anomalously high values of U_{10} that we were not able to reproduce in this study. The impact of this finding is tremendous because the data in error were used to derive ocean surface drag parameterization in WRF, the most widely used numerical weather prediction model (Davis, Wang, et al., 2008). This parameterization was later used by many (Davis, Jones, & Riemer, 2008; Davis et al., 2010; Nolan et al., 2009; Gopalakrishnan et al., 2012; Cavallo et al., 2013; Green & Zhang, 2013, 2014). Further, the original data informed and influenced subsequent lines of research (Takagaki et al., 2012, 2016; Chen et al., 2007, 2013), and was influential enough to be covered by review papers (Black et al., 2007; Sullivan & McWilliams, 2010). It is thus important to reflect back on the literature since the original publication of the drag saturation data, with the new understanding that the absolute magnitudes of drag coefficient have been underestimated. However, the key finding of drag saturation by Donelan et al. (2004) remains, and is further supported by this study.

As a further step of verification of stress and wave data between this study and Donelan et al. (2004), we compare the power spectra of wave elevation at 9-m fetch and four different levels of high wind speed (Fig. 5). The spectral peak progressively shifts toward lower frequencies with higher winds. The sheltering of short waves is evidenced by a dip in the wave energy immediately to the right of the windsea peak, between 2 and 3 Hz, likely due to the air-flow separation in the lee of the dominant waves. This process has been observed in the laboratory using particle-image velocimetry (Reul et al., 1999; Buckley & Veron, 2016, 2019), and was proposed by Donelan et al. (2004)

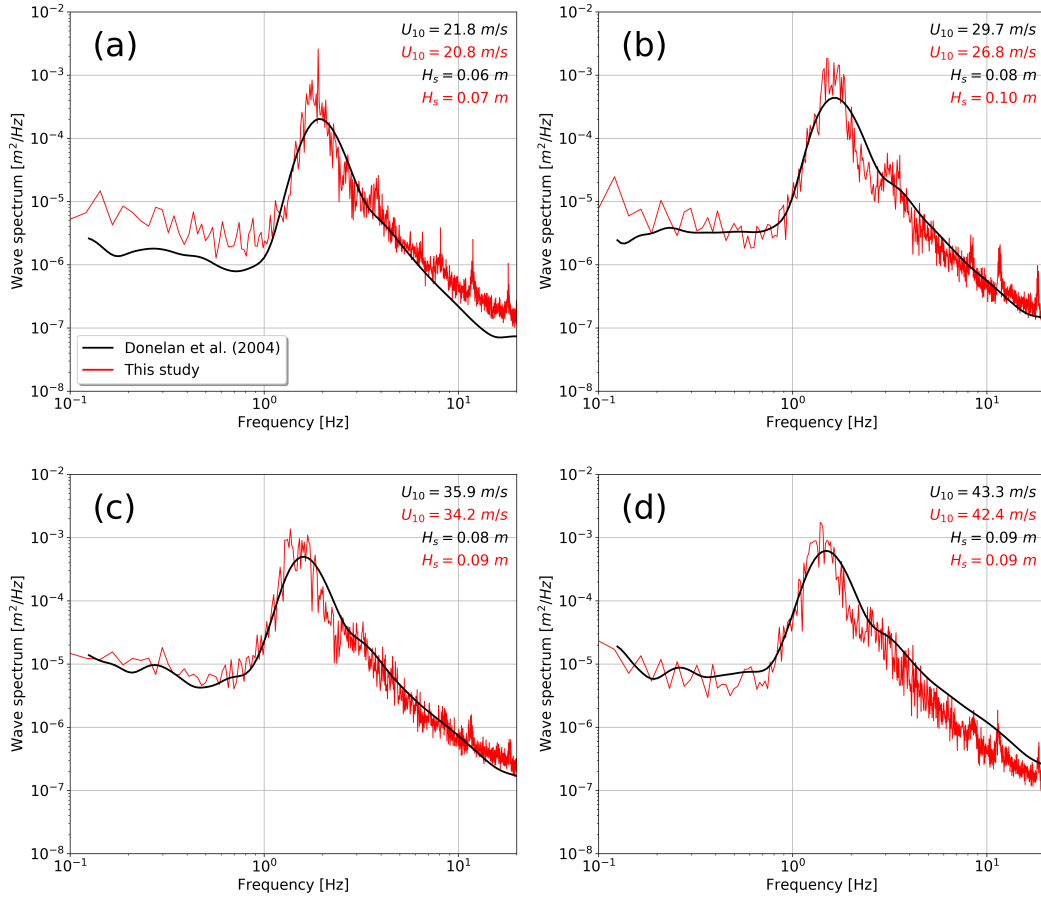


Figure 5. Measured wave elevation spectra at 9-m fetch in moderate-to-high wind conditions, from Donelan et al. (2004) in black and this study in red. 10-m wind and significant wave height values are shown in the upper-right corner of each panel.

as the dominant mechanism behind drag saturation. At very high wind speeds, most of the momentum input occurs at the peak wave, which dissipates and downshifts some of its energy, as evidenced by the increase in wave energy for $f < 1$ Hz (Fig. 5b, c, d). Long waves shelter shorter waves and limit their growth, and at the same time dissipate due to direct impact from wind. The former process acts to reduce the drag, the latter to increase it. The spectra from Donelan et al. (2004), based on laser elevation gauge data, are in close agreement with our own, which validates the high-speed camera imaging method for non-intrusive measurement and analysis of wave spectra.

It is imperative to remember that the wind and wave conditions in the laboratory are not equivalent to those in the open ocean. Limitations include constrained water depth, fetch, directional spread wind-generated waves, as well as the air space between the water and the ceiling of the tank. Great care thus must be taken when designing experiments, collecting and analyzing measurements, and interpreting the results. Nevertheless, wind-wave laboratories provide an invaluable framework in which the forcing conditions, as well as the measurement instrumentation can be controlled at an unprecedented degree. Such measurements are challenging, and often even impossible to collect in the field.

5 Conclusions

We conclude with several key points and recommendations:

1. New laboratory data from the momentum budget method and eddy-covariance flux measurements from two different instruments show further evidence of air-sea drag saturation in strong winds, in both fresh and seawater.
2. The new drag estimates agree with the field observations (Edson et al., 2013) in low-to-moderate winds ($U_{10} < 25 \text{ m s}^{-1}$), and lab measurements (Donelan et al., 2004; Takagaki et al., 2012) in high winds ($U_{10} > 25 \text{ m s}^{-1}$).
3. During the momentum budget analysis, we discovered a programming error in the original source code used to generate drag estimates by Donelan et al. (2004). The error caused the incorrect wind speed data array to be used when scaling the wind speed and drag coefficient to a reference 10-m height.
4. Correction to the 10-m wind speed estimates from the dataset of Donelan et al. (2004) yields 10-m drag coefficients that agree better with field data in low-to-moderate winds by Edson et al. (2013). The revised drag saturates at $U_{10} \approx 29 \text{ m s}^{-1}$, at a level of $C_D \approx 3.1 \times 10^{-3}$. This saturation level corresponds to a 34% increase relative to the original estimates, with saturation occurring at 12% lower wind speed threshold.
5. Laboratory measurements of drag in high winds over short fetch must be cautiously compared to field measurements, due to the limitation of wind-wave tanks to develop wave states comparable to those in the open ocean. Drag parameterizations derived from such experiments (Donelan et al., 2004; Takagaki et al., 2012, 2016), as well as this study, should be used mindfully and cautiously when implementing into numerical weather prediction models such as WRF (Powers et al., 2017) or MPAS (Skamarock et al., 2012, 2018).
6. This work illustrates that not only are weather and ocean prediction models vulnerable to programmer errors, but that the datasets and analyses from which parameterization schemes are derived may contain errors as well. There is thus an increasing level of urgency to adopt open data, open software, and open science practices across the theoretical, observational, and numerical modeling disciplines.
7. Further work is needed to bridge the gap between the wind and wave conditions in the open ocean and those that can be recreated in the laboratory. The next step in this line of work will yield wind, wave, and drag measurements in the 23-m long SUSTAIN wave flume at the University of Miami, capable of generating extreme-force (Category 5 hurricane) winds. These experiments will also explore the role of background wave conditions on drag, such as complex spectra that are found in the open ocean.

Acknowledgments

We thank all members of the SUSTAIN laboratory at the University of Miami who helped with the set up and calibration of instruments and data acquisition. Discussions with William Drennan, Nathan Laxague, and Andrew Smith helped improve this study. The data and code to reproduce the figures in this manuscript can be downloaded at <https://github.com/sustain-lab/Curcic-Haus-2020>. The original data and code by Donelan et al. (2004) can be downloaded at <https://github.com/sustain-lab/HIDRAG>. This work was supported by the National Science Foundation grant number 1745384.

References

- Andreas, E. L. (1992). Sea spray and the turbulent air-sea heat fluxes. *Journal of Geophysical Research: Oceans*, 97(C7), 11429–11441.

- Bell, M. M., Montgomery, M. T., & Emanuel, K. A. (2012). Air–sea enthalpy and momentum exchange at major hurricane wind speeds observed during cblast. *J. Atmos. Sci.*, *69*(11), 3197–3222.
- Black, P. G., D’Asaro, E. A., Drennan, W. M., French, J. R., Niiler, P. P., Sanford, T. B., ... Zhang, J. A. (2007). Air–sea exchange in hurricanes: Synthesis of observations from the coupled boundary layer air–sea transfer experiment. *Bull. Amer. Met. Soc.*, *88*(3), 357–374.
- Buckley, M. P., & Veron, F. (2016). Structure of the airflow above surface waves. *J. Phys. Oceanogr.*, *46*(5), 1377–1397.
- Buckley, M. P., & Veron, F. (2019). The turbulent airflow over wind generated surface waves. *European Journal of Mechanics-B/Fluids*, *73*, 132–143.
- Cavallo, S. M., Torn, R. D., Snyder, C., Davis, C., Wang, W., & Done, J. (2013). Evaluation of the advanced hurricane wrf data assimilation system for the 2009 atlantic hurricane season. *Mon. Wea. Rev.*, *141*(2), 523–541.
- Chassignet, E. P., Hurlburt, H. E., Smedstad, O. M., Halliwell, G. R., Hogan, P. J., Wallcraft, A. J., ... Bleck, R. (2007). The HYCOM (HYbrid Coordinate Ocean Model) data assimilative system. *Journal of Marine Systems*, *65*(1-4), 60–83.
- Chen, S. S., & Curcic, M. (2016). Ocean surface waves in hurricane ike (2008) and superstorm sandy (2012): Coupled model predictions and observations. *Oce. Mod.*, *103*, 161–176.
- Chen, S. S., Price, J. F., Zhao, W., Donelan, M. A., & Walsh, E. J. (2007). The cblast-hurricane program and the next-generation fully coupled atmosphere–wave–ocean models for hurricane research and prediction. *Bull. Amer. Met. Soc.*, *88*(3), 311–318.
- Chen, S. S., Zhao, W., Donelan, M. A., & Tolman, H. L. (2013). Directional wind–wave coupling in fully coupled atmosphere–wave–ocean models: Results from cblast-hurricane. *J. Atmos. Sci.*, *70*(10), 3198–3215.
- Collins, C., Potter, H., Lund, B., Tamura, H., & Graber, H. (2018). Directional wave spectra observed during intense tropical cyclones. *J. Geophys. Res.: Oceans*, *123*(2), 773–793.
- Curcic, M., Chen, S. S., & Özgökmen, T. M. (2016). Hurricane-induced ocean waves and stokes drift and their impacts on surface transport and dispersion in the gulf of mexico. *Geophys. Res. Lett.*, *43*(6), 2773–2781.
- Davis, C. A., Jones, S. C., & Riemer, M. (2008). Hurricane vortex dynamics during atlantic extratropical transition. *J. Atmos. Sci.*, *65*(3), 714–736.
- Davis, C. A., Wang, W., Chen, S. S., Chen, Y., Corbosiero, K., DeMaria, M., ... Xiao, Q. (2008). Prediction of Landfalling Hurricanes with the Advanced Hurricane WRF Model. *Mon. Wea. Rev.*, *136*(6), 1990–2005. doi: 10.1175/2007MWR2085.1
- Davis, C. A., Wang, W., Dudhia, J., & Torn, R. (2010). Does increased horizontal resolution improve hurricane wind forecasts? *Weather and Forecasting*, *25*(6), 1826–1841.
- Donelan, M. A. (2018). On the decrease of the oceanic drag coefficient in high winds. *Journal of Geophysical Research: Oceans*, *123*(2), 1485–1501.
- Donelan, M. A., Dobson, F. W., Smith, S. D., & Anderson, R. J. (1993). On the dependence of sea surface roughness on wave development. *J. Phys. Oceanogr.*, *23*(9), 2143–2149. doi: 10.1175/1520-0485(1993)023(2143:OTDOSS)2.0.CO;2
- Donelan, M. A., Drennan, W. M., & Katsaros, K. B. (1997). The airsea momentum flux in conditions of wind sea and swell. *J. Phys. Oceanogr.*, *27*(10), 2087–2099. doi: 10.1175/1520-0485(1997)027(2087:TASMFI)2.0.CO;2
- Donelan, M. A., Haus, B. K., Plant, W. J., & Troianowski, O. (2010). Modulation of short wind waves by long waves. *J. Geophys. Res.: Oceans*, *115*(C10).
- Donelan, M. A., Haus, B. K., Reul, N., Plant, W. J., Stiassnie, M., Graber, H. C., ... Saltzman, E. S. (2004). On the limiting aerodynamic rough-

- ness of the ocean in very strong winds. *Geophys. Res. Lett.*, *31*(18). doi: 10.1029/2004GL019460
- Edson, J. B., Hinton, A. A., Prada, K. E., Hare, J. E., & Fairall, C. W. (1998). Direct covariance flux estimates from mobile platforms at sea. *Journal of Atmospheric and Oceanic Technology*, *15*(2), 547–562.
- Edson, J. B., Jampana, V., Weller, R. A., Bigorre, S. P., Plueddemann, A. J., Fairall, C. W., ... Hersbach, H. (2013). On the exchange of momentum over the open ocean. *J. Phys. Oceanogr.*, *43*(8), 1589–1610.
- Gopalakrishnan, S. G., Goldenberg, S., Quirino, T., Zhang, X., Marks Jr, F., Yeh, K.-S., ... Tallapragada, V. (2012). Toward improving high-resolution numerical hurricane forecasting: Influence of model horizontal grid resolution, initialization, and physics. *Weather and Forecasting*, *27*(3), 647–666.
- Green, B. W., & Zhang, F. (2013). Impacts of air–sea flux parameterizations on the intensity and structure of tropical cyclones. *Mon. Wea. Rev.*, *141*(7), 2308–2324.
- Green, B. W., & Zhang, F. (2014). Sensitivity of tropical cyclone simulations to parametric uncertainties in air–sea fluxes and implications for parameter estimation. *Mon. Wea. Rev.*, *142*(6), 2290–2308.
- Holthuijsen, L. H., Powell, M. D., & Pietrzak, J. D. (2012). Wind and waves in extreme hurricanes. *J. Geophys. Res.: Oceans*, *117*(C9).
- Hsu, J.-Y., Lien, R.-C., D’Asaro, E. A., & Sanford, T. B. (2019). Scaling of drag coefficients under five tropical cyclones. *Geophys. Res. Lett.*
- Jarosz, E., Mitchell, D. A., Wang, D. W., & Teague, W. J. (2007). Bottom-up determination of air–sea momentum exchange under a major tropical cyclone. *Science*, *315*(5819), 1707–1709.
- Jeong, D., Haus, B. K., & Donelan, M. A. (2012). Enthalpy transfer across the air–water interface in high winds including spray. *J. Atmos. Sci.*, *69*(9), 2733–2748.
- Large, W., & Pond, S. (1981). Open ocean momentum flux measurements in moderate to strong winds. *J. Phys. Oceanogr.*, *11*(3), 324–336.
- Laxague, N. J., Curcic, M., Björkqvist, J.-V., & Haus, B. K. (2017). Gravity-capillary wave spectral modulation by gravity waves. *IEEE Transactions on Geoscience and Remote Sensing*, *55*(5), 2477–2485.
- Nolan, D. S., Zhang, J. A., & Stern, D. P. (2009). Evaluation of planetary boundary layer parameterizations in tropical cyclones by comparison of in situ observations and high-resolution simulations of hurricane isabel (2003). part i: Initialization, maximum winds, and the outer-core boundary layer. *Mon. Wea. Rev.*, *137*(11), 3651–3674.
- Ortiz-Suslow, D. G., Haus, B. K., Mehta, S., & Laxague, N. J. (2016). Sea spray generation in very high winds. *J. Atmos. Sci.*, *73*(10), 3975–3995.
- Phillips, O. M. (1966). *The dynamics of the upper ocean*. Cambridge University Press.
- Potter, H., Graber, H. C., Williams, N. J., Collins III, C. O., Ramos, R. J., & Drennan, W. M. (2015). In situ measurements of momentum fluxes in typhoons. *J. Atmos. Sci.*, *72*(1), 104–118.
- Powell, M. D., Vickery, P. J., & Reinhold, T. A. (2003). Reduced drag coefficient for high wind speeds in tropical cyclones. *Nature*, *422*(6929), 279.
- Powers, J. G., Klemp, J. B., Skamarock, W. C., Davis, C. A., Dudhia, J., Gill, D. O., ... Duda (2017). The weather research and forecasting model: Overview, system efforts, and future directions. *Bull. Amer. Met. Soc.*, *98*(8), 1717–1737. doi: 10.1175/BAMS-D-15-00308.1
- Reul, N., Branger, H., & Giovanangeli, J.-P. (1999). Air flow separation over unsteady breaking waves. *Physics of Fluids*, *11*(7), 1959–1961.
- Sanford, T. B., Price, J. F., & Girton, J. B. (2011). Upper-ocean response to hurricane frances (2004) observed by profiling em-apex floats. *J. Phys. Oceanogr.*,

- 41(6), 1041–1056.
- Shchepetkin, A. F., & McWilliams, J. C. (2005). The regional oceanic modeling system (roms): a split-explicit, free-surface, topography-following-coordinate oceanic model. *Ocean modelling*, 9(4), 347–404.
- Skamarock, W. C., Duda, M. G., Ha, S., & Park, S.-H. (2018). Limited-area atmospheric modeling using an unstructured mesh. *Mon. Wea. Rev.*, 146(10), 3445–3460.
- Skamarock, W. C., Klemp, J. B., Duda, M. G., Fowler, L. D., Park, S. H., & Ringler, T. D. (2012). A multiscale nonhydrostatic atmospheric model using centroidal voronoi tessellations and c-grid staggering. *Mon. Wea. Rev.*, 140(9), 3090–3105.
- Soloviev, A. V., Lukas, R., Donelan, M. A., Haus, B. K., & Ginis, I. (2014). The air-sea interface and surface stress under tropical cyclones. *Scientific reports*, 4, 5306.
- Sullivan, P. P., & McWilliams, J. C. (2010). Dynamics of winds and currents coupled to surface waves. *Annual Review of Fluid Mechanics*, 42, 19–42.
- Takagaki, N., Komori, S., Suzuki, N., Iwano, K., Kuramoto, T., Shimada, S., ... Takahashi, K. (2012). Strong correlation between the drag coefficient and the shape of the wind sea spectrum over a broad range of wind speeds. *Geophys. Res. Lett.*, 39(23). doi: 10.1029/2012GL053988
- Takagaki, N., Komori, S., Suzuki, N., Iwano, K., & Kurose, R. (2016). Mechanism of drag coefficient saturation at strong wind speeds. *Geophys. Res. Lett.*, 43(18), 9829–9835. doi: 10.1002/2016GL070666
- Tennekes, H., Lumley, J. L., Lumley, J., et al. (1972). *A first course in turbulence*. MIT press.
- Wright, C. W., Walsh, E., Vandemark, D., Krabill, W., Garcia, A., Houston, S., ... Marks, F. (2001). Hurricane directional wave spectrum spatial variation in the open ocean. *J. Phys. Oceanogr.*, 31(8), 2472–2488.